Biomass Conversion and Biorefinery
https://doi.org/10.1007/s13399-021-02222-1

ORIGINAL ARTICLE

One-pot production of thermostable PHB biodegradable polymer by co-producing bio-melanin pigment in engineered *Escherichia coli*

SeoA Park[1] · Yung-Hun Yang[2] · Kwon-Young Choi[1,3]

Received: 6 August 2021 / Revised: 7 December 2021 / Accepted: 10 December 2021

Abstract

In this study, to engineer a polyhydroxybutyrate (PHB) biopolymer, pyomelanin pigment was coproduced in a single *Escherichia coli* host and incorporated into PHB. The cells convert l-tyrosine into pyomelanin via the formation of homogentisate by expressing hydroxyphenylpyruvate dioxygenase (*hppd*), while producing PHB by expressing *bktB*, *phaB*, and *phaC* simultaneously. Up to 0.52 ± 0.16 g/L of sum of pyomelanin and PHB is produced, and its mixture (5.7% w/w) was emulsified in DMSO solution for pyoPHB film formation after sonication-induced nucleation of pyomelanin. To characterize the newly generated pyoPHB film, its color diagram, radical scavenging capacity, thermostability, and volume resistance are determined. The melting temperature and decomposition enthalpy increased in pyoPHB by 12%, and the antioxidant activity of the pyoPHB film increased by 16% compared to those of the control PHB film. Although the volume resistivity increased by more than 10 times, it is still within that of commercial plastics. Interestingly, more than 200 mg/L of pyomelanin could be stably produced in the co-producing host even though the PHB content was up to 50% level of cell mass and expression level of *hppd* was decreased by co-expression of PHB synthetic genes, which was estimated to be attributed to increased ATP pools. Therefore, finally, the ATP concentration in each of the pyomelanin- and PHB-producing cells was determined, resulting in a significant increase (up to fivefold) in the co-producing strain.

Keywords PHB · Pyomelanin · Bio pigments · Thermostability · Engineered PHB · Co-production

1 Introduction

Petroleum-based plastics are cost-effective, lightweight, durable, and have good properties for commercial applications [1]. However, the recycling rate of plastic is very low at approximately 9%, and nontreated or discarded plastics are released into the environment by incineration or from landfills [2]. These discarded petroleum-based plastics cause problems in the environment and ecosystems. Recently, interest in eco-friendly materials has increased, with strategies of plastic waste upcycling and the development of plastic alternatives being explored in the drive for carbon neutrality in the plastic industry. In particular, there is an increasing interest in biodegradable materials that can be applied to biodegradable polymers. One promising candidate is polyhydroxyalkanoates (PHA), which are a group of nontoxic, biocompatible, and biodegradable biopolymers [3, 4]. In particular, PHAs can be produced through microbial fermentation and extracted from PHA-producing cells, contrary to other biodegradable polymers, such as polylactic acid, polybutylene succinate (PBS), and polybutylene adipate terephthalate, which currently requires additional chemical polymerization [5, 6]. Polyhydroxybutyrate (PHB), the most common form of PHA with a short side chain, has physical properties similar to those of polypropylene [7]. It has relatively high crystallinity and lower impact strength than other biodegradable polymers [8]. In addition, it has a low

✉ Yung-Hun Yang
seokor@konkuk.ac.kr

✉ Kwon-Young Choi
kychoi@ajou.ac.kr

[1] Department of Environmental Engineering, College of Engineering, Ajou University, Suwon, Gyeonggi-do, South Korea

[2] Department of Biological Engineering, College of Engineering, Konkuk University, 120 Neungdong-ro, Gwanngjin-gu, Seoul 05029, Republic of Korea

[3] Department of Environmental and Safety Engineering, College of Engineering, Ajou University, Suwon, Gyeonggi-do, South Korea

Published online: 27 January 2022

decomposition temperature of approximately 220 °C relative to its melting point of 175–180 °C [9, 10].

However, several limitations must yet be overcome to commercialize PHAs as biodegradable polymers. First, their mechanical properties should be improved according to the purpose of the polymer [11]. Rather, it may be necessary to mix it with other useful ingredients in the form of a composite to slow or control the degree of biodegradation. Alternatively, various functionalities may be provided to the PHA polymers through the generation of such composites. Recently, our group reported the coproduction of PHA polymers with indigo dyes, which resulted in the formation of a blue-colored PHA (bcPHA) biopolymer [12]. This process included a one-pot biosynthesis of bcPHA in a single cell with the supply of indole and glucose bioresources. Although no dramatic increase in its thermostability or physiological activities was observed, the preparation of a high-performance PHA polymer through the coproduction of functional biomaterials is promising.

Melanin is a group of pigments found in the biosphere. It is synthesized through a series of random polymerizations between repeating units of radicals, and its coloring is commonly brown to black. It is divided into eumelanin, pheomelanin, neuromelanin, allomelanin, and pyomelanin according to its color and synthetic route [13–15]. Melanin has been reported to not only block ultraviolet rays but also possess physiological properties such as anti-oxidant, anti-tumor, and anti-bacterial effects [16, 17]. In addition, melanin has been reported to exhibit high thermal stability (up to 300 °C) and emit a strong exothermic peak at 700 °C [18]. Furthermore, the redox properties of melanin pigments have enabled their use in electrical materials such as electrodes, supercapacitors, and semiconducting materials [19, 20]. Because of these characteristics, increasing efforts have been made to apply melanin as a cosmetic, bio-sorbent, and bio-adhesive with diverse functionalities [21]. However, the application of melanin in biodegradable PHB polymer composite was not common. Previously, Kiran et al. reported the synthesis of nanomelanin-PHB composite film and its protective effect against *Staphylococcus aureus* [22]. They produced melanin using *Pseudomonas* sp. and blended it with PHB after nanomelanin particle formation through sonication. The nanomelanin-PHB composite showed thermostability up to 281.87 °C and a high protective effect against *S. aureus*. In addition, melanin was also applied to several synthetic polymers such as polypropylene (PP) and polyethylene terephthalate (PET). For example, dopamine-modified clay was incorporated in PP polymer with melanin-oriented excellent radical scavenging capacity [23]. Also, it was used for a PET coating material, which showed interesting polymeric and optical properties [24].

While eumelanin has received considerable attention, pyomelanin, which is synthesized through l-tyrosine aminotransferase- and hydroxyphenylpyruvate dioxygenase (*hppd*)-dependent multi-reactions, has not been characterized [13–16]. Recently, our group established a heterologous production of pyomelanin biopolymer using 4-hydroxyphenylpyruvate dioxygenase isolated from *Ralstonia pickettii* in *Escherichia coli*, which had interesting characteristics of antioxidant capacity and unique particle morphology [14].

In this study, pyomelanin was simultaneously produced in a PHB-producing *E. coli* strain. The cells co-expressed *hppd* and *phaBC*-encoding genes for the biosynthesis of pyomelanin and PHB, respectively. The PHB formed a composite with pyomelanin to generate a black-colored pyoPHB (pyomelanin + PHB), which is estimated to possess both physical properties of PHB and pyomelanin with increased thermostability. To verify this, thermal stability was determined using differential scanning calorimetry (DSC) analysis. The electrical conductivity was measured to verify the applicability of the films as electrical materials. Finally, the visible characteristics of the pyoPHB film surfaces were investigated through an SEM image analysis. The findings represent a development in the chemical and physical properties of PHB biodegradable polymers and advance their commercial viability.

2 Materials and methods

2.1 Chemicals and reagents

The *Ralstonia pickettii* strain was isolated from soil and it was verified to produce pyomelanin previously [14]. l-Tyrosine, dimethylsulfoxide (DMSO), 2, 2′-azino-bis(3-ethylbenzothiazoline-6-sulfonic acid) (ABTS), and M9 minimal salt 5 × were purchased from Sigma-Aldrich Korea (Suwon, Gyeonggi-do, South Korea). Luria–Bertani (LB) and nutrient broth (NB) were purchased from Difco (Difco Korea, Seoul).

2.2 Bacterial strains and culture condition

The PHB-producing strains and plasmids used in this study were obtained from a previous study [12]. Briefly, *E. coli* KSYH(DE3) harboring pLW487::*bktB*::*phaB*::*phaC* plasmid was used as host strains for PHB production. Pyomelanin synthetic gene of *hppd* derived from *Ralstonia pickettii* was cloned into the pET-28a(+) vector and expressed in *E. coli* (BL21). The *hppd*-expressing *E. coli* cells were incubated in M9 minimal medium supplemented with 2 mM l-tyrosine [14]. The cells were incubated at 37 °C until OD_{600} reached 0.8, and then IPTG (0.25 mM) was added for induction. The cells were further incubated at 30 °C to produce pyomelanin. Pyomelanin pigment production was observed and quantified hourly. For the production of PHB, the cells were

similarly incubated in M9 minimal medium supplemented with 2% glucose at 37 °C until OD_{600} reached 0.8, and then IPTG (0.25 mM) was added for induction. After then, the cells were further incubated at 30 °C to produce PHB. For co-production of pyomelanin and PHB, the same cell culture with both l-tyrosine and glucose and induction method were applied.

2.3 Extraction of pyomelanin and PHB

To purify the generated pyomelanin pigments localized extracellularly, the growth medium was collected through centrifugation for 15 min at 8000 rpm, and the supernatant was treated with 6 M HCl to adjust the pH to 2.0 for pyomelanin precipitation. After 4 h of incubation, the precipitated pyomelanin was collected by centrifugation for 15 min at 8000 rpm. The extracted crude pyomelanin was washed with distilled water three times, and the pyomelanin powder was prepared by drying at 60 °C for 24 h [25]. To extract PHB located intracellularly, cells were collected by centrifugation at 8000 rpm for 15 min and washed twice with deionized H_2O. After removing the supernatant for pyomelanin extraction and drying the collected cells in a dry oven, the dry cell mass was measured by weighing it in a glass vial. The cell pellets were resuspended in water and lyophilized. For methanolysis of PHB, 1 mL of chloroform and 1 mL of a methanol/sulfuric acid (85:15 v/v) mixture were added to the cell [26, 27]. It was incubated at 100 °C for 2.5 h, followed by cooling on ice for 10 min. Then, 1 mL of ice-cold distilled water was added, and the sample was thoroughly vortexed. The organic phase (bottom) was separated and prepared for PHB film formation.

2.4 Pretreatment of pyomelanin and preparation of pyomelanin-incorporated PHB (pyoPHB) film

To prepare pyomelanin-incorporated PHB (pyoPHB) film, pyomelanin was first sonicated to form a nanoparticle through nucleation and ensure that pyomelanin was evenly mixed with PHB, it was sonicated at 20% amplitude for a total of 7 min by pulsing for 8 s, and resting for 10 s. DMSO solvent was added to nanoparticle pyomelanin and PHB extract mixture and dissolved at 150 °C for 1 h to obtain a homogenous solution [28]. The mixed solution was dried and solidified at 100 °C to obtain pyoPHB film. For a single PHB film preparation, the same protocol except pyomelanin pretreatment step was applied.

2.5 Quantitative analysis of pyomelanin and PHB

Quantitative analysis of pyomelanin was performed using HPLC (Younglin, South Korea) and spectrometric analyses [14]. The HPLC was equipped with a UV detector and reverse phase C18 column (Zorbax extend C18 Waters, 250 nm × 4.6 nm, 3.5 µm, Agilent, USA). An isocratic scheme with 7:3 of water (0.1% TFA): acetonitrile (0.1% TFA) solvent ratio was applied for elution. The column temperature was set at 30 °C during separation. The flow rate was set as 1 mL/min and the eluent absorbance was monitored at 254 nm. To analyze isolated PHB quantitatively, gas-chromatography (Younglin, Seoul, South Korea) was used. Agilent's DB-FFAP (30 m × 0.25 mm) was used for the gas chromatography column. The oven temperature increased by a rate of 10 °C/min to 100 °C, 20 °C/min to 220 °C, and 10 °C/min to 230 °C for 3, 5, and 5 min, respectively. N_2 gas was used as the carrier gas, the temperature was set at 210 °C, and the flow rate was 3 mL/min. The flame ionization detection temperature was set to 230 °C.

2.6 Determination of antioxidant activity

The radical scavenging capacity was measured using an ABTS method. The reaction solution was prepared by mixing ABTS solution in PBS buffer (14.8 mM) and potassium persulfate solution in distilled water (4.9 mM) at a 1:1 ratio. After mixing both solutions, the pH was adjusted to 7.4, and the reaction was initiated by adding sunlight-blocked films. After 24 h of incubation, the reaction mixture was diluted with distilled water up to an optical density of approximately 0.7. The absorbance of the final solution was monitored at OD_{734}, and the ABTS scavenging capacity was calculated by the equation: relative activity (%) = $[(A_{control} - A_{sample})/A_{control}] \times 100$ (%) [29].

2.7 Determination of color difference of films

The color difference was measured using a colorimeter JZ-600 instrument (Shenzhen Kingwell Instrument Co., Ltd., Guangdong, China) and analyzed using color analysis management software. The color differences were measured using color meter units of $\Delta E^*_{ab} = [(\Delta L^*)^2 + (\Delta a^*)^2 + (\Delta b^*)^2]^{½}$, where ΔL^*, brightness, the closer to +, the lighter, the closer to -, the darker; Δa^*, the closer to +, the redder, the closer to -, the greener; Δb^*, the closer to +, the yellower, the closer to -, the bluer. $\Delta E^*_{ab} = [(\Delta L^*)^2 + (\Delta a^*)^2 + (\Delta b^*)^2]^{½}$

2.8 Differential scanning calorimeter (DSC) and scanning electron microscopy (SEM) analysis of pyoPHB and control PHB films

DSC analysis for specific heat capacity measurement was performed using DSC 204 F1 Phoenix (NETZSCH, Wittelsbacherstraße 42, Germany), and the T_m value was obtained by increasing the temperature from 0 to 300 °C at a rate of 10 °C/min. And SEM image analysis was performed using a JSM-7900F field emission scanning electron microscope/

energy dispersive X-Ray spectrometer (JEOL Ltd., Tokyo, Japan), and film surfaces were observed at × 1000 and × 5000 magnification.

2.9 Determination of volume resistivity of pyoPHB and control PHB films

Volume resistivity of pyoPHB and control PHB films was conducted according to the ASTM D257 standard test method. The MCP-HT800 (Nittoseiko Analytech Co., Ltd., Kanagawa, Japan) high resistance meter was used. The resistance ranges were from 103 to 1016 Ω and the probe was UR100. The measurements were conducted at 23 ± 2 °C and 50 ± 5% of room humidity.

2.10 Determination of ATP concentration in PHB and pyoPHB producing strains.

For quantification of ATP concentration in PHB and pyoPHB producing strains, an ATP assay kit (DogenBio Kit, Seoul, South Korea) was used. Briefly, 1 mM standard solution by mixing 10 µL of ATP standard solution (10 mM) and 90 µL of distilled water was prepared for calibration. Each 10 mg of samples was suspended in 100 µL of ATP assay buffer. After adding 2 to 50 µL of the prepared samples to a 96 well plate, the final volume was adjusted to 50 µL using the assay buffer. Each reaction mixture included 44 µL of ATP assay buffer, 2 µL of ATP enzyme mix, 2 µL of ATP converter, and 2 µL of ATP probe. Then, 50 µL of samples was mixed with the 50µL of the reaction mixture. After reacting for 30 min at room temperature where the light is blocked, its absorbance was read at 570 nm with gently shaking. ATP concertation in the sample (C) was calculated by $C = B/VD$ (nmol/µL), where B is the ATP amount of measurement in well (nmol), V is the amount of sample dispensed into the well (µL), and D is the sample dilution factor.

3 Results and discussion

3.1 Construction of pyomelanin and PHB coproduction host strain

Pyomelanin was synthesized by *tyrB* and *hppd* enzyme reactions from l-tyrosine. As TyrB enzyme, a class of aromatic amino acid aminotransferase, was expressed in the *E. coli* host cells endogenously, the *hppd* encoding gene was introduced into the host and expressed heterologously. In PHB synthesis, the *bktB*, *phaB*, and *phaC* genes in the PHB synthetic pathway were expressed, and both pyomelanin synthetic gene and PHB synthetic genes were co-expressed for coproduction of pyomelanin and PHB (Fig. 1a).

3.2 Production of pyomelanin and PHBs

For pyomelanin and PHB production, each l-tyrosine and glucose were fed as a carbon source into the medium. As controls, independently synthesized pyomelanin by *hppd*-expressing cells and PHB films by *bktB*-, *phaB*-, and *phaC*-expressing cells were prepared, respectively. Using the recombinant production hosts, pyomelanin and PHB were produced separately or simultaneously, and their production was quantitatively analyzed. According to our previous report on pyomelanin production, a single expression of *hppd* could result in approximately 315 mg/L of pyomelanin production in *E. coli*, whereas additional expression of *bktB* and *phaBC* led to a decrease in pyomelanin production of 214.4 ± 17.9 mg/L with 30.7 ± 4.3 mg/g cells of production yield per cell mass (Fig. 1b). This was estimated to be attributed to the co-production of PHB in a single host. However, maintaining the 70% production level was quite meaningful considering co-expression of multiple genes and lowered expression level of *hppd* gene in the host cell. In contrast, the production of PHB was not greatly affected by the co-expression of *the hppd* gene. The control *bktB*- and *phaBC*-expressing cells produced 0.73 ± 0.22 g/g cells of PHB, while 0.49 ± 0.16 g/g PHB could be obtained from the cells expressing both PHB synthetic genes and pyomelanin synthetic gene.

3.3 Preparation and colorimetric analysis of biosynthetic PHB and pyoPHB films

Next, pyomelanin-incorporated PHB (pyoPHB) film was prepared by dissolving both in DMSO solution. Before homogenization in the solution, the isolated pyomelanin was sonicated to form a nanoparticle through nucleation and ensure that pyomelanin was evenly mixed with PHB, followed by emulsified homogenization at 150 °C. The emulsified solution with 5.7% w/w of pyomelanin content was dried at room temperature and prepared for pyoPHB film formation (Fig. 2a). Control PHB films without pyomelanin were prepared as the same procedure for comparison (Fig. 2b). Each 10 × 10 cm PHB film was prepared and the coloration of pyoPHB was measured by colorimetry (Fig. 2c). Coloration factors were quantitively determined and a comparable ΔE_{ab} was calculated (Table 1). As was visibly observed, pyoPHB showed a deep brown coloration with 30.61 L and an a^* brightness. However, the dyeing performance and brightness were not evenly controlled because of the nonhomogeneous and viscous characteristics of the PHB film during drying and solidification. Although all processes were conducted in a one-pot biosynthesis, an additional process for homogenized conditions during solidification would be necessary to obtain high-quality pyoPHB films.

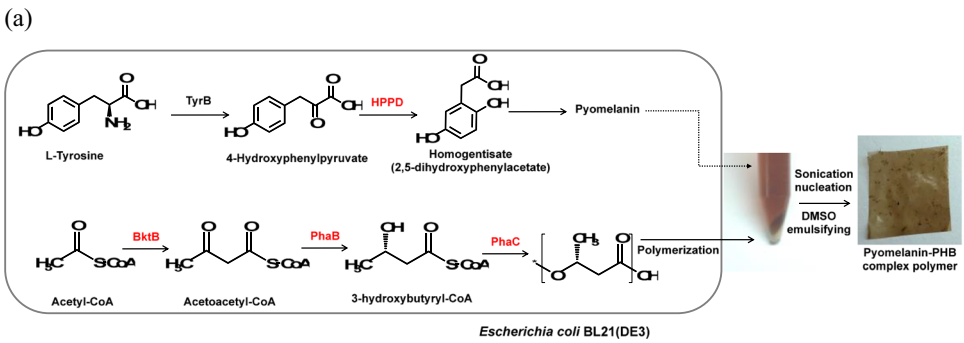

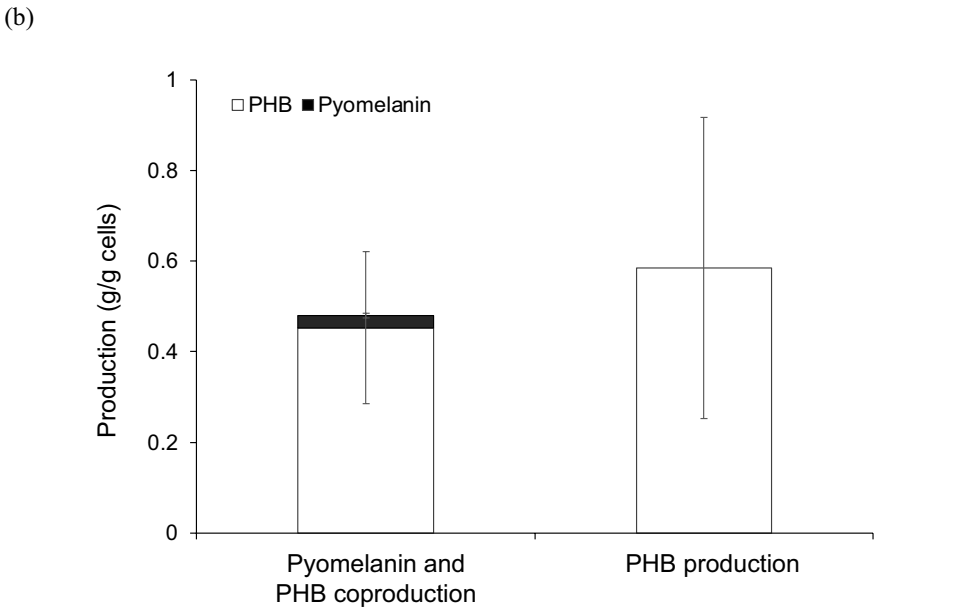

Fig. 1 **a** Biosynthesis of PHB and pyomelanin in a single host strain and procedure for preparation of pyomelanin-incorporated PHB (pyoPHB) film. **b** Production titer of pyomelanin and PHB in pyomelanin and PHB co-production host and single PHB production host at the same condition

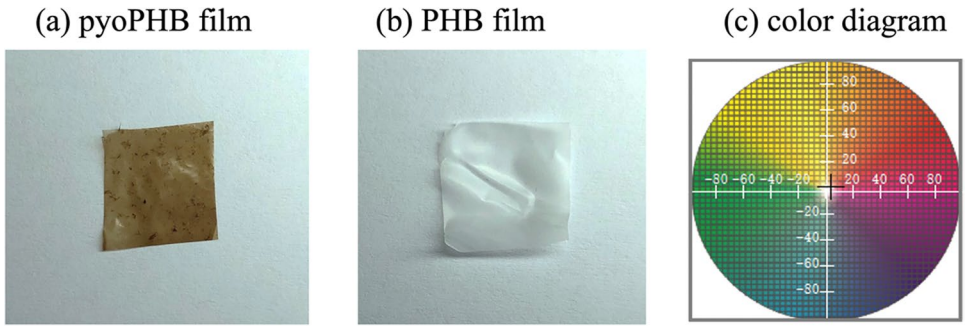

Fig. 2 The produced **a** pyoPHB film and **b** biosynthetic control PHB film (in order). **c** Colorimeter image and position of the pyoPHB film in the color diagram

Table 1 Color differences of PHB and pyoPHB films

Samples	ΔL^*	Δa^*	Δb^*	ΔE^*
PHB	92.79	−1.56	−2.86	-
pyoPHB	30.61	4.49	5.62	62.31

ΔL^*, brightness, the closer to +, the lighter, the closer to -, the darker; Δa^*, the closer to +, the redder, the closer to -, the greener; Δb^*, the closer to +, the yellower, the closer to -, the bluer. $\Delta E^*_{ab} = [(\Delta L^*)^2 + (\Delta a^*)^2 + (\Delta b^*)^2]^{1/2}$

3.4 Surface analysis of biosynthetic control PHB film and pyoPHB films by SEM

Next, SEM image analysis was conducted to investigate the pyoPHB surface and compare it with the control PHB film. Surprisingly, the surfaces of PHB without pyomelanin incorporation and pyoPHB film showed obvious differences in the × 1000 analysis. The surface of the control

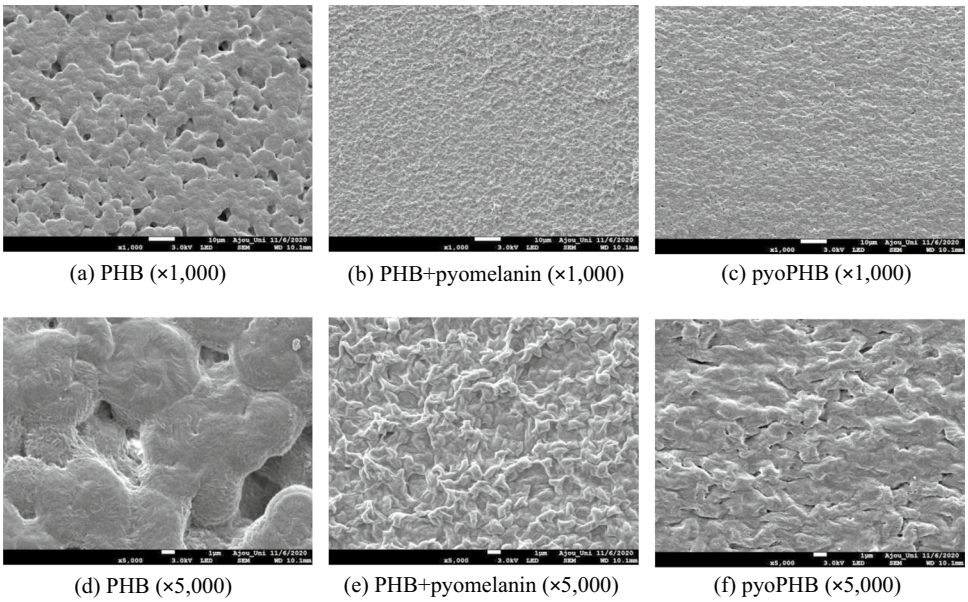

(a) PHB (×1,000) (b) PHB+pyomelanin (×1,000) (c) pyoPHB (×1,000)

(d) PHB (×5,000) (e) PHB+pyomelanin (×5,000) (f) pyoPHB (×5,000)

Fig. 3 SEM images showing biosynthetic PHB film and PHB + pyomelanin film as controls, and pyoPHB film crystals at **a**–**c** × 1000, and **d**–**f** × 5000 magnification

PHB possessed micropores that were randomly distributed and entangled (Fig. 3a and d), whereas the surfaces of PHB + pyomelanin (Fig. 3b and 3e) and pyoPHB (Fig. 3c and d) did not have micropores. Rather, both pyomelanin incorporated PHB surfaces showed a flat but relatively rough surface covered with regular packing. Also, the surface of pyoPHB displayed more regularly packed rather than PHB + pyomelanin control. This suggested that the intracellular interaction between synthesized pyomelanin and PHB might affect its incorporation mechanisms, thereby resulting in tightly packed morphology rather than by mixing of pyomelanin and PHB obtained separately. The inner micropores in the PHB surface could be observed clearly by expanded surface analysis at × 5000, whereas pyoPHB seems tightly packed (Fig. 3d–f).

From this observation, we estimate that pyoPHB has a higher crystallinity and is denser than the PHB films. The higher packing and tighter organization in the pyoPHB film might change the related physical properties. Therefore, several physical properties, such as radical scavenging capacity, thermostability, and volume resistivity, were investigated.

3.5 Antioxidant activities of biosynthetic control PHB and pyoPHB films

Previous reports regarding the antioxidant activities of natural and synthetic melanin pigments found that their radical scavenging capacity ranged within 100–200 mg/mL, equivalent to several times that of ascorbic acid as a control. Previously, our group reported the antioxidant activity of a microbial pyomelanin isolated from *Ralstonia rikettii*. The IC_{50} value against ABTS was determined as 108.9 μg/mL [14]. Considering natural and synthetic melanins, in which the capacities were observed to range from 126.8 to 284 μg/mL [30], pyomelanin could be an excellent candidate as an antioxidant ingredient for PHB films. To verify the antioxidant capacity of pyoPHB, an ABTS assay was performed against PHB and pyoPHB films, and the relative antioxidant activity in terms of removal efficiency was determined. The control PHB film showed only 1.9% radical scavenging activity, while pyoPHB showed much higher activity of 18.3% (Fig. 4). This result is promising as the antioxidant functionality could be mounted on the PHB biodegradable film by incorporating pyomelanin pigment during PHB biosynthesis.

3.6 DSC analysis of pyoPHB and control PHB films

Next, DSC analysis was performed to investigate the changes in the thermostability of the PHB films by incorporating

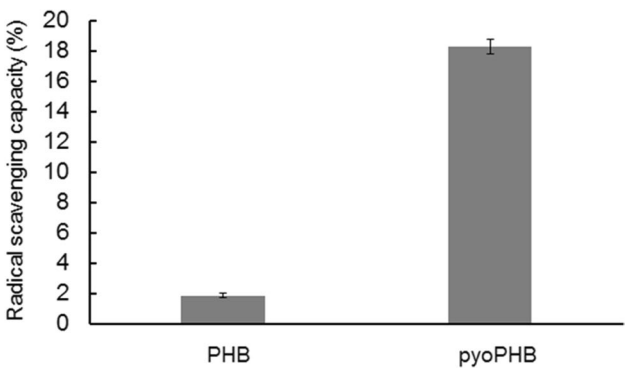

Fig. 4 Radical scavenging capacities of control PHB film and pyoPHB films

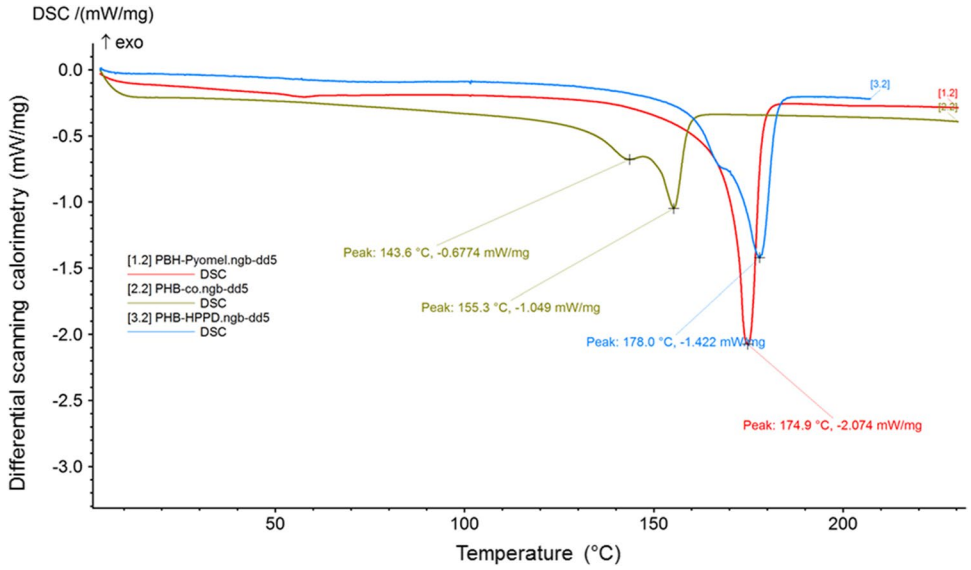

Fig. 5 DSC curves of PHB (green), PHB + pyomelanin mixture (red), and pyoPHB films (blue)

pyomelanin. Here, in addition to control PHB film without pyomelanin, additional control PHB film which was prepared by mixing PHB and pyomelanin after being synthesized separately by different production host as the same procedures for comparison. The incorporated pyomelanin content was set as same with 5.7% w/w. The melting temperatures of PHB, PHB-pyomelanin mixture and pyoPHB film were determined as 155.3, 174.9, and 178.0 °C, respectively. Two endothermic melting peaks were observed in the normal PHB film and pyoPHB film, which may be ascribed to the melt crystallization theory. In particular, the characteristic melting temperature was increased by incorporating pyomelanin into the PHB film, suggesting that pyomelanin affects global organization and morphology (Fig. 5).

The addition of pyomelanin into the PHB film via simple mixing was also effective. Of course, the thermostability would be dependent on the amount of pyomelanin used in the PHB film mixture; the same concentration of pyomelanin, which could be produced by the pyoPHB-producing strain, was used for accurate comparison. However, the pyoPHB film prepared in a single host was the most effective for obtaining high thermostability, suggesting that pyomelanin production in the PHB and pyomelanin coproducing strain is critical for thermostability control. The enthalpy values calculated from DSC analysis revealed that the highest value of − 102.4 J/g was obtained for the pyoPHB film, suggesting that the pyoPHB film absorbs the heat to be transferred to PHB instead and requires more heat to decompose (Table 2). Although the exact incorporation of pyomelanin during polymerization was not clearly understood here, the unidentified interaction in pyomelanin and PHB biosynthesis and incorporation in a single host might affect its crystallization and thermal stability rather than by simple mixing of pyomelanin and PHB.

Table 2 DSC curves data of control PHB, PHB + pyomelanin films, and comparison with pyomelanin-incorporated pyoPHB film

Sample	T_{m1} (◦C)	T_{m2} (◦C)	Δ*H* (J/g)
PHB	146.3	155.3	− 75.51
PHB + pyomelanin[a]	-	174.9	− 94.31
pyoPHB	167.3	178.0	− 102.4

[a]PHB film which was prepared by mixing PHB and pyomelanin after being synthesized separately by different production hosts as the same procedure

Table 3 Electrical conductivity of films

Samples		Thickness (mm)	Volume resistivity of a material (Ω cm)
PHB	Average	0.019	3.59×10^{16}
	SD	-	8.16×10^{15}
	CV (%)	-	22.77
pyoPHB	Average	0.263	2.44×10^{15}
	SD	-	3.36×10^{14}
	CV (%)	-	13.78

SD, standard deviation; *CV*, coefficient of variation = (SD/average) × 100

3.7 Volume resistivity of biosynthetic control PHB and pyoPHB films

Melanin has also been used as an electrical insulator and capacitor [31]. To investigate the electrical properties of the PHB films, each PHB film (10 cm × 10 cm) was prepared, and their volume resistivity values were determined (Table 3). As results, both PHB and pyoPHB showed very

low volume resistivity values at 3.59×10^{16} and 2.44×10^{15} Ω cm, respectively, which are within the values of typical high-molecular materials such as commercial plastics (Table 3). In general, the electrical resistivity of a material with an electrical conductivity of less than 10^5 S cm^{-1} and a resistance value of approximately 10^{16} Ω cm, such as pyoPHB and PHB, would be useful as insulating materials in further application. Although the pyomelanin-incorporated structure was not suitable for use as electrical materials in this study due to its heterogeneity and disorder, several engineering strategies such as the precise design of the ordered structure and adopting modification building blocks during its random polymerization would be challenging.

3.8 Determination of ATP concentration in PHB and pyoPHB producing cells

In cells, the generation of PHA is triggered by the intracellular concentration ratio of phosphate, especially ATP [32]. PHA is a good reservoir for the catabolism of volatile fatty acids through the incorporation of polyphosphate into ATP [33]. Interestingly, more than 200 mg/L of pyomelanin could be stably produced in the co-producing host even though the PHB content was up to 50% level of cell mass and expression level of *hppd* was decreased by co-expression of PHB synthetic genes, which was estimated to be attributed to increased ATP pools. Previously, co-production of PHB was reported to increase cell mass and glucose utilization, thereby resulting in increased heterologous production of isobutanol [34]. To verify the correlation between PHB overproduction and cell mass production, the intracellular ATP concentration was determined. *E. coli* cells expressing empty vectors were used as a control, and ATP concentration increased by up to 60% in PHB-producing cells, while it was decreased by 40% in pyomelanin-producing cells. Interestingly, the cells coproducing PHB and pyomelanin showed five times higher intracellular ATP concentrations than the control cells (Fig. 6). It was surprising that PHB production affected cellular energy and could enhance the heterogenous metabolites by increasing cell mass. To verify the interaction, a more in-depth study is required in the future.

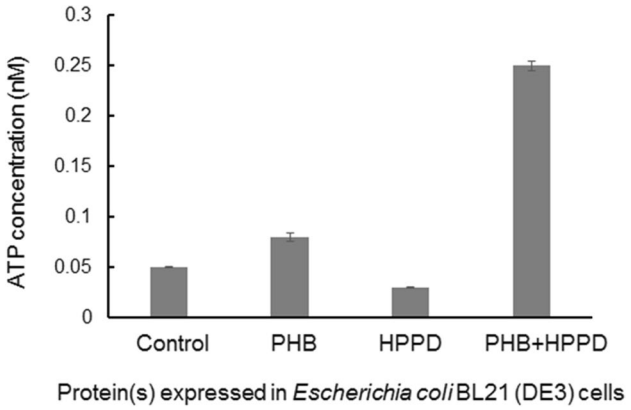

Fig. 6 ATP concentrations in PHB, HPPD, and PHB + HPPD expressing cells

4 Conclusion

In this study, pyomelanin was co-produced by expressing the HPPD enzyme in PHB-producing host cells. The cells could produce 0.52 ± 0.16 g/g cells of pyoPHB polymer which showed characteristic properties. Moreover, a co-production of pyomelanin and PHB has great advantages of high thermostability and surface morphology in a consolidated bioprocess of single-cell culture and extraction process. Otherwise, independent two biotransformations with different optimization processes are inevitable. The pyoPHB film showed a higher melting temperature than that of the PHB film and exhibited significantly increased antioxidant activity. Owing to the incorporation of pyomelanin into PHB micropores, pyoPHB could have a less amorphous surface structure and related thermostability as well. Although the electrical resistivity of pyoPHB increased by approximately 15 times that of PHB, it was within the range of 10^{16} Ω cm, which needs further intensive improvement for electrical applications. More interestingly, the pyoPHB-producing *E. coli* host showed five times higher intracellular ATP concentrations. However, additional research would be necessary for a better understanding of the interaction between PHB and related cellular metabolisms. In conclusion, PHA biopolymers are very promising materials that can be further utilized as their monomers can be produced and polymerized simultaneously in wild-type or engineered microorganisms, suggesting that a complete consolidated bioprocess can be implemented. However, PHA biopolymers must be further developed to obtain more desirable physical properties if they are to be commercially viable and practical plastic alternatives. Accordingly, the results obtained in this study would provide a foundation for further related research.

Author contribution K-Y. Choi and Y-H. Yang conceptualized and designed the study, and S. Park conducted the pyoPHA experiments and analyzed biopolymer data. And K-Y. Choi, Y-H. Yang, and S. Park wrote the manuscript.

Funding This work was supported by the National Research Foundation of Korea (NRF) grant, funded by the Ministry of Education, Science, and Technology (MEST) (2021R1A2C1007519).

Declarations

Ethics approval This article does not contain any studies with human participants performed by any of the authors.

Conflict of interest The authors declare no competing interests.

References

1. North EJ, Halden RU (2013) Plastics and environmental health: the road ahead. Rev Environ Health 28:1–8
2. Geyer R, Jambeck JR, Law KL (2017) Production, use, and fate of all plastics ever made. Sci Adv 3:e1700782
3. Muller-Santos M, et al. (2020). The protective role of PHB and its degradation products against stress situations in bacteria. FEMS Microbiol Rev:fuaa058.
4. Mosnackova K et al (2020) Properties and degradation of novel fully biodegradable PLA/PHB blends filled with keratin. Int J Mol Sci 21:9678
5. McAdam B et al (2020) Production of polyhydroxybutyrate (PHB) and factors impacting its chemical and mechanical characteristics. Polymers (Basel) 12:2908
6. Munir S, Jamil N (2020) Polyhydroxyalkanoate (PHA) production in open mixed cultures using waste activated sludge as biomass. Arch Microbiol 202:1907–1913
7. Holmes PA (1985) Applications of PHB-a microbially produced biodegradable thermoplastic. Phys Technol 16:1
8. Padermshoke A et al (2005) Melting behavior of poly(3-hydroxybutyrate) investigated by two-dimensional infrared correlation spectroscopy. Spectrochim Acta A Mol Biomol Spectrosc 61:541–550
9. Anbukarasu P, Sauvageau D, Elias A (2015) Tuning the properties of polyhydroxybutyrate films using acetic acid via solvent casting. Sci Rep 5:17884
10. Yeo JCC et al (2018) Recent advances in the development of biodegradable PHB-based toughening materials: approaches, advantages and applications. Mater Sci Eng C Mater Biol Appl 92:1092–1116
11. Martinez-Herrera RE et al (2020) Efficient recovery of thermostable polyhydroxybutyrate (PHB) by a rapid and solvent-free extraction protocol assisted by ultrasound. Int J Biol Macromol 164:771–782
12. Jung H-R et al (2020) Production of blue-colored polyhydroxybutyrate (PHB) by one-pot production and coextraction of indigo and PHB from recombinant *Escherichia coli*. Dyes Pigm 173:107889
13. Wang Z et al (2020) Melanin produced by the fast-growing marine bacterium *Vibrio natriegens* through heterologous biosynthesis: characterization and application. Appl Environ Microbiol 86:e02749-e2819
14. Seo D, Choi K-Y (2020) Heterologous production of pyomelanin biopolymer using 4-hydroxyphenylpyruvate dioxygenase isolated from *Ralstonia pickettii* in *Escherichia coli*. Biochem Eng J 157:107548
15. Jang S et al (2018) FCS and ECH dependent production of phenolic aldehyde and melanin pigment from l-tyrosine in *Escherichia coli*. Enzyme and Microb Technol 112:59–64
16. Patra V, Gallais Serezal I, Wolf P (2020) Potential of skin microbiome, pro- and/or pre-biotics to affect local cutaneous responses to UV exposure. Nutrients 12:1795
17. Ruan L et al (2004) Melanin pigment formation and increased UV resistance in *Bacillus thuringiensis* following high temperature induction. Syst Appl Microbiol 27:286–289
18. Sajjan SS, Anjaneya O, Kulkarni Guruprasad B, Nayak Anand S, Mashetty Suresh B, Karegoudar TB (2012) Properties and functions of melanin pigment from Klebsiella sp. GSK. Kor J Microbiol Biotechnol 41:60–69
19. Kwon IS et al (2016) In vitro electrochemical characterization of polydopamine melanin as a tissue stimulating electrode material. J Mater Chem B 4:3031–3036
20 Park H et al (2020) Engineering of melanin biopolymer by co-expression of MelC tyrosinase with CYP102G4 monooxygenase: structural composition understanding by 15 tesla FT-ICR MS analysis. Biochem Eng J 157:107530
21. SeoA Park CL, Lee J, Jung S, Choi K-Y (2020) Applications of natural and synthetic melanins as biosorbents and adhesive coatings. Biotechnol Bioprocess Eng 35:646–654
22. Kiran GS et al (2017) Synthesis of Nm-PHB (nanomelanin-polyhydroxy butyrate) nanocomposite film and its protective effect against biofilm-forming multi drug resistant Staphylococcus aureus. Sci Rep 7:9167
23. Phua SL et al (2013) Simultaneous enhancements of UV resistance and mechanical properties of polypropylene by incorporation of dopamine-modified clay. ACS Appl Mater Interfaces 5:1302–1309
24. Jeon JR, Le TT, Chang YS (2016) Dihydroxynaphthalene-based mimicry of fungal melanogenesis for multifunctional coatings. Microb Biotechnol 9:305–315
25. Yang YH et al (2012) Biosynthesis of poly(3-hydroxybutyrate-co-3-hydroxyvalerate) containing a predominant amount of 3-hydroxyvalerate by engineered Escherichia coli expressing propionate-CoA transferase. J Appl Microbiol 113:815–823
26. Balakrishna Pillai A, Jaya Kumar A, Kumarapillai H (2018) Enhanced production of poly(3-hydroxybutyrate) in recombinant *Escherichia coli* and EDTA-microwave-assisted cell lysis for polymer recovery. AMB Express 8:142
27. Andler R et al (2021) Synthesis of poly-3-hydroxybutyrate (PHB) by *Bacillus cereus* using grape residues as sole carbon source. International Journal of Biobased Plastics 3:98–111
28. Aramvash A, Moazzeni Zavareh F, Gholami Banadkuki N (2018) Comparison of different solvents for extraction of polyhydroxybutyrate from *Cupriavidus necator*. Eng Life Sci 18:20–28
29. Park SA, S.-Y.A., and Kwon-Young Choi, (2020) Functional microbial pigments isolated from *Chryseobacterium* and *Deinococcus* species for bio-paint application. Biotechnol Bioprocess Eng 25:394–402
30. Ahn S-Y et al (2019) Synthesis and chemical composition analysis of protocatechualdehyde-based novel melanin dye by 15T FT-ICR: high dyeing performance on soft contact lens. Dyes Pigm 160:546–554
31. Ambrico M et al (2011) Melanin layer on silicon: an attractive structure for a possible exploitation in bio-polymer based metal-insulator-silicon devices. Adv Mater 23:3332–3336
32. Third KA, Newland M, Cord-Ruwisch R (2003) The effect of dissolved oxygen on PHB accumulation in activated sludge cultures. Biotechnol Bioeng 82:238–250
33. Vu DH et al (2021) Production of polyhydroxyalkanoates (PHAs) by *Bacillus megaterium* using food waste acidogenic fermentation-derived volatile fatty acids. Bioengineered 12:2480–2498
34. Song HS et al (2020) Enhanced isobutanol production by co-production of polyhydroxybutyrate and cofactor engineering. J Biotechnol 320:66–73